The Astronomical Journal, 167:270 (11pp), 2024 June https://doi.org/10.3847/1538-3881/ad40ae

Age Analysis of Extrasolar Planets: Insight from Stellar Isochrone Models

C. Swastik[1,2], Ravinder K. Banyal[1], Mayank Narang[3,4], Athira Unni[1,5], and T. Sivarani[1]
[1] Indian Institute of Astrophysics, Koramangala 2nd Block, Bangalore 560034, India; swastik.chowbay@iiap.res.in
[2] Pondicherry University, R.V. Nagar, Kalapet, 605014, Puducherry, India
[3] Department of Astronomy and Astrophysics, Tata Institute of Fundamental Research Homi Bhabha Road, Colaba, Mumbai 400005, India
[4] Academia Sinica Institute of Astronomy & Astrophysics, 11F of Astro-Math Bldg., No. 1, Sec. 4, Roosevelt Road, Taipei 10617, Taiwan, Republic of China
[5] Department of Physics and Astronomy, University of California, Irvine, 4129 Frederick Reines Hall, Irvine, CA 92697, USA
Received 2024 March 11; revised 2024 April 16; accepted 2024 April 16; published 2024 May 17

Abstract

There is growing evidence from stellar kinematics and galactic chemical evolution suggesting that giant planets ($M_P \geqslant 0.3 M_J$) are relatively young compared to the most commonly occurring population of small planets ($M_P < 0.3 M_J$). To further test the validity of these results, we analyzed the ages for a large number of 2336 exoplanet hosting stars determined using three different but well-established isochrone fitting models, namely, PARSEC, MIST, and Yonsei Yale. As input parameters, we used Gaia DR3 parallaxes, magnitudes, and photometric temperature, as well as spectroscopically determined more accurate temperatures and metallicities from the Sweet Catalog. Our analysis suggests that ∼50%–70% of stars with planets are younger than the Sun. We also find that, among the confirmed exoplanetary systems, stars hosting giant planets are even younger compared to small planet hosts. The median age of ∼2.61–3.48 Gyr estimated for the giant planet-hosting stars (depending on the model input parameters) suggests that the later chemical enrichment of the galaxy by the iron-peak elements, largely produced from Type Ia supernovae, may have paved the way for the formation of gas giants. Furthermore, within the giant planet population itself, stars hosting hot Jupiters (orbital period ⩽10 days) are found to be younger compared to the stellar hosts of cool and warm Jupiters (orbital period >10 days), implying that hot Jupiters could be the youngest systems to emerge in the progression of planet formation.

Unified Astronomy Thesaurus concepts: Stellar ages (1581); Exoplanet formation (492); Planet hosting stars (1242); Extrasolar gaseous giant planets (509); Exoplanets (498); Hot Jupiters (753)

1. Introduction

The field of exoplanets has seen a rapid rise in the past three decades after the discovery of the first planet by Mayor & Queloz (1995). We realized that planets are ubiquitous and their architecture and properties are considerably more diverse and complex (Carter et al. 2012; Gaudi et al. 2017; Gillon et al. 2017; Zhu & Dong 2021). Apart from the strange planet discovered around the pulsar: PSR1257 + 12 (Wolszczan & Frail 1992), the earliest exoplanets discovered were all giants, equivalent to Jupiter in mass and size. Among those initial discoveries were hot Jupiters which orbit their stars with periods of a few days as they were easier to detect compared to smaller planets (Mayor & Queloz 1995; Charbonneau et al. 2000; Henry et al. 2000). Thus, the first exoplanet detection, is itself a surprise to the astronomy community since no such planet exists in our solar system. Numerous revelations have emerged over the years since the first discovery. To date, more than 5000 exoplanets have been discovered, which span a wide range of population. While some planets orbit in close proximity to their parent star (MacDonald et al. 2016; Mills et al. 2016; Barragán et al. 2018; Malavolta et al. 2018; Smith et al. 2018; Lam et al. 2021), others have incredibly extended orbits (Naef et al. 2001; Tamuz et al. 2008; Chauvin 2018; Benisty et al. 2021; Vigan et al. 2021; Wahhaj et al. 2021; Currie et al. 2023; Ren et al. 2023; Wahhaj et al. 2024).

Several correlations connecting the stellar and planetary properties have emerged in the past decade (Santos et al. 2004; Fischer & Valenti 2005; Fischer et al. 2014; Narang et al. 2018; Sousa et al. 2021; Swastik et al. 2021; Unni et al. 2022). One such correlation is the stellar age–planetary-mass correlation. The ages of stars with planets (SWP) are crucial for investigating numerous aspects of planetary system evolution, such as dynamical interactions among planets (Laughlin & Chambers 2002) and tidal effects generated by SWP (Pätzold et al. 2004; Barker & Ogilvie 2009). In fact, understanding the ages of stars holds significant importance in the process of selecting stellar candidates for planet detection (Bonfanti et al. 2015) and assessing their potential habitability. The rotation and activity levels of a star which serve as indicators of stellar age, play a crucial role in determining the habitability of planets orbiting around them.

The majority of planets have been detected around main-sequence FGK stars. Due to the degeneracy of parameters and the slow evolution of stars in main-sequence, it is difficult to accurately constrain the ages of these stars. Owing to the ambiguities inherent in estimating age, greater precision is required for these investigations. Unlike other stellar properties, such as $T_{\rm eff}$, log g and [Fe/H], ages cannot be directly observed or measured. To estimate stellar ages, one uses an indirect model-dependent technique such as isochrone fitting (Valls-Gabaud 2014). Other approaches, such as gyrochronology and activity index, are also used in addition to isochrone fitting from stellar evolutionary models. Chemical analysis (also known as chemiochronology; Delgado Mena et al. 2019; Swastik et al. 2022) and stellar kinematics (Binney et al. 2000; Wu et al. 2021) can be used to estimate the ages of an ensemble

of stars but cannot be used for individual cases. Asteroseismology stands as the sole method capable of ascertaining the age of a star with an impressive level of precision, reaching uncertainties as low as ∼11% (Bellinger et al. 2019). However, it requires longer time-series data, which is only accessible for a limited sample of stars. Additionally, it only applies to stars hotter than about spectral type K, as cooler stars do not typically exhibit the oscillations required for estimating ages using asteroseismology (Silva Aguirre et al. 2015; Christensen-Dalsgaard & Aguirre 2018). Each of the aforementioned models requires input parameters derived from various sources. Each input parameter is accompanied by its own uncertainty, which ultimately propagates into the age estimation.

The ages of the individual planet-hosting stars are often determined using different models and input parameters. Due to the inherent uncertainties associated with each model and its input parameters, carrying out a meaningful statistical comparison becomes challenging. There have been limited homogeneous studies for the ages of the planet-hosting stars. Early studies such as Saffe et al. (2005) have estimated the stellar ages of the 49 planets hosting stars. Since the sample was very small, it was not possible to draw any robust conclusions about different populations of planets. Recent studies of 326 planets hosting stars by Bonfanti et al. (2015) using PARSEC isochrones have found that ∼6% of stars have ages lower than 0.5 Gyr, while ∼7% of stars are older than 11 Gyr. Additionally, their results showed that the majority of their planet-hosting stars fall within the age range of 1.5–2 Gyr, indicating a prevalence of younger systems. Using astroseismology data for 33 Kepler exoplanet host stars, Silva Aguirre et al. (2015) have found that the majority of these Kepler host stars are older than the Sun. Further study of 335 transiting planets hosting stars by Bonfanti et al. (2016) has shown that the median age of the sample is ∼5 Gyr, which is similar to the solar age. These studies motivated us to look for possible correlations between stellar ages and planet mass. However, these studies are based on a limited sample of stars, and the ages derived in these papers have strong dependence on the models and input parameters. As a result, the estimates become less reliable for studying any statistical correlation between the stellar ages and the properties of their planetary companions.

In order to understand how stellar ages are correlated with planetary properties, we need to analyze a large number of planet-hosting stars with minimal errors in their ages. Because of the difficulties in getting precise age estimates from isochrone models due to high uncertainties, we confirmed these estimates using established isochrone fitting models and parameters from photometric and spectroscopic data. Our findings indicate that, while slight variations in age estimates may occur based on the specific input parameters or models employed, the overall statistical trends for a large sample of planet-hosting stars remain unchanged. In this study, our specific objective is to determine the ages of stars that host planets and examine the relationships between stellar ages and planetary properties, namely, the orbital period and mass of the exoplanets. We used combinations of input parameters from photometry and spectroscopy and three isochrone fitting models (MESA Isochrones & Stellar Tracks; MIST; Choi et al. 2016; Dotter 2016; PAdova and tRieste Stellar Evolutionary Code; PARSEC; Bressan et al. 2012; q2-Yonsei-Yale; YY; Han et al. 2009; Ramírez et al. 2014) for the analysis. The paper is organized as follows. In Section 2 we describe our sample of stars hosting planets. Section 3 discusses the methodology of the age determination using isochrones. In Sections 4 and 5 we discuss the trends for stellar ages as a function of planet mass and interpret the results in terms of the chemical evolution of our galaxy. Finally, we summarize and conclude our findings in Section 6.

2. Sample Selection

To study the dependence of stellar ages on planetary properties such as planet mass (M_P) and orbital period, we selected an initial sample of 3775 planet-hosting stars from the NASA exoplanet archive (Akeson et al. 2013; NASA Exoplanet Science Institute 2020). To calculate stellar ages using isochrone fitting techniques, we need accurate stellar parameters from spectroscopy (such as $T_{\rm eff}$, log g, and [Fe/H]), photometry (like G-band magnitude), and astrometry (like parallax, proper motion, etc). The photometric and astrometric data was obtained from GAIA observations by cross matched[6] our sample with GAIA DR3 (Gaia Collaboration et al. 2023), while for the spectroscopic data was obtained from the sweet-cat (Andreasen et al. 2017; Sousa et al. 2018, 2021), which is a catalog of stellar parameters for SWP determined homogeneously from spectroscopy. We narrowed down our analysis to main-sequence stars due to the complexities associated with accounting for evolutionary effects, such as photospheric mixing, which can introduce variations in photospheric metallicities (Bergemann et al. 2011; Swastik et al. 2022). Subsequently, we excluded super-Jupiters ($M_P \geqslant 5M_J$) and multiplanetary systems hosting at least one small planet ($M_P < 0.3M_J$) and a giant planet ($M_P \geqslant 0.3M_J$), as including such multiplanetary systems would make it difficult to discern differences in stellar populations between small and giant planets as multiplanetary systems show properties similar to giant planets and are statistically younger (see Appendix B of Swastik et al. 2022). The distinction between small and giant planets is taken at the mass of Saturn, drawing on the mass-density rationale presented in Hatzes & Rauer (2015). This boundary is based on the observed shift in the slope within the mass-density relationship for exoplanets. Further, Bashi et al. (2017) used mass–radius relations and arrived at similar conclusions. They further suggested that the location of the breakpoint is linked to the onset of electron degeneracy in hydrogen, and therefore to the planetary bulk composition. For further analysis, we retained only those stars that have age uncertainties smaller than their main-sequence lifetime, as recommended by Pont & Eyer (2004). Additionally, we excluded lower main-sequence stars ($T_{\rm eff} < 4400$ K) from our sample since the main-sequence lifetime for such stars can exceed the age of the universe, and, therefore, the current stellar isochrone models cannot reliably estimate their age. Consequently, our final data set comprised 2336 stars hosting 3034 planets (see Table 1).

3. Stellar Age Determination: Isochrones

To determine the ages from isochrone, one places the star on the Hertzsprung−Russell diagram (HRD) with $T_{\rm eff}$ on the x-axis and luminosity L on the y-axis (Figure 1). The $T_{\rm eff}$ and L

[6] Initially, we used a wider search radius, but in this instance, a 3″ search radius was adequate to retrieve all planet-hosting stars. We also used other sources, such as the SIMBAD, to confirm that they are actual planet-hosting stars.

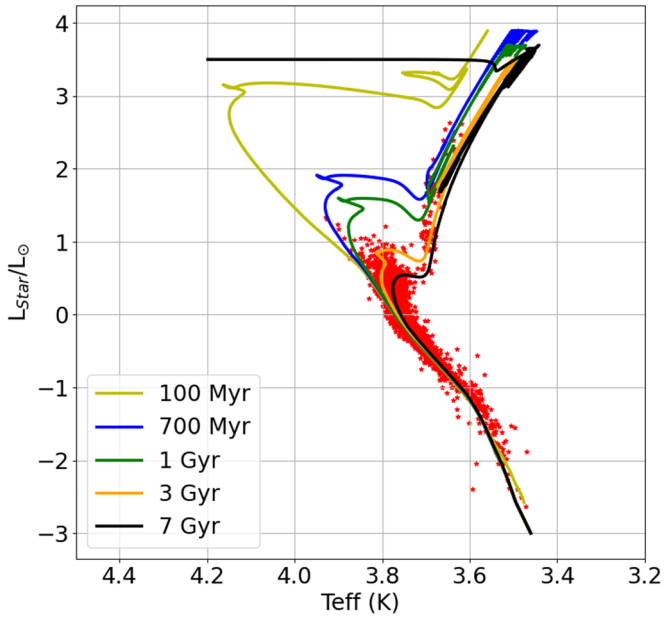

Figure 1. Stellar isochrone models generated using MIST. The red symbols represent planet-hosting stars. The isochrones are drawn for the solar-scaled abundances. Both X and Y scales are in logarithmic units.

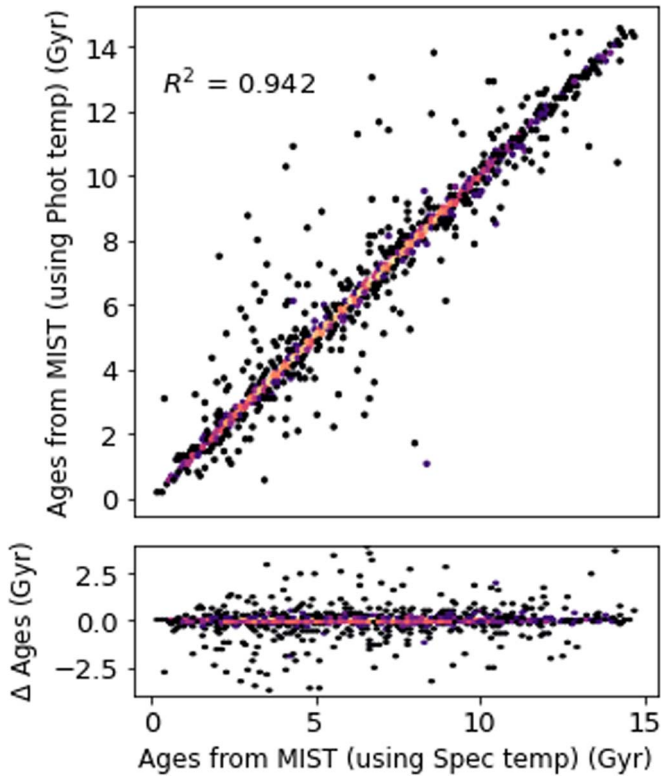

Figure 2. Comparison of stellar ages computed from photometric $T_{\rm eff}$ from Gaia DR3 and spectroscopic $T_{\rm eff}$ from sweet-cat. The color coding represents the density of points.

can be obtained by several techniques. In the case of $T_{\rm eff}$, it can be determined both by spectroscopy and photometry (color-index), while the L is computed from the observed total flux, which is obtained from the photometric magnitude (Rodrigo et al. 2017), and distance from the parallax (π). These observables have their own intrinsic errors and systematics

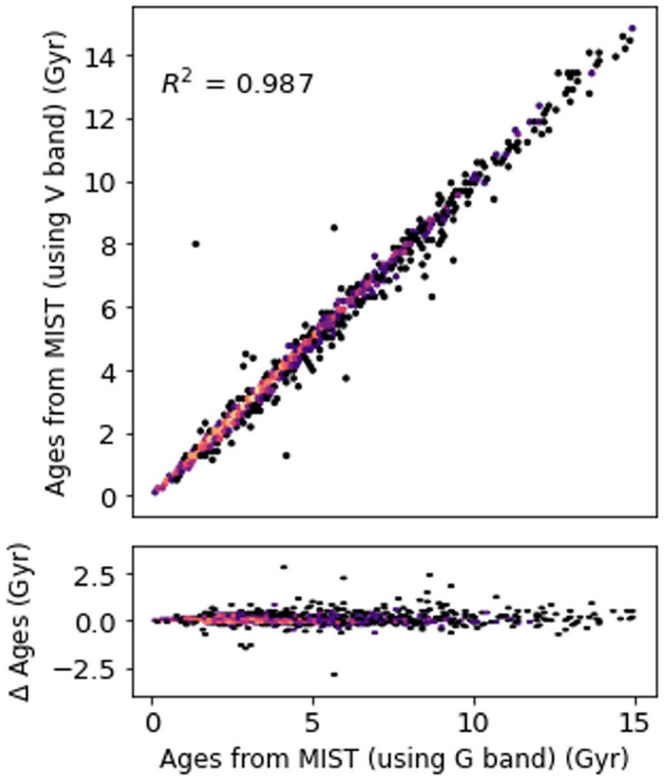

Figure 3. Comparison of stellar ages from MIST model using *V*-band (Johnson) and *G*-band (Gaia) mag. The color coding represents the density of stars.

based on the techniques used to obtain them. Thus, the isochrone placement technique becomes challenging to determine the ages of a star with high accuracy. Further, for the lower main-sequence stars ($T_{\rm eff} < 4400$ K), the isochrone ages are not reliable as the evolution timescales for these stars are > age of the universe, and thus it becomes challenging to model the evolution of such systems.

Another factor that influences the determination of isochrone ages is the selection of models/grids. While different isochrone models share a common goal of estimating stellar ages, they diverge in their underlying assumptions. For instance, the equation of state (EOS) employed by the PARSEC models primarily relies on the Free EOS tool.[7] In contrast, MIST and YY isochrones predominantly utilize the Opacity Project at Livermore (Iglesias & Rogers 1996) and the Stewart–Colwell–Vasil–Helfand equation of state (Saumon et al. 1995), respectively. Furthermore, variations in solar abundances among the different isochrone models contribute to discrepancies in their results. For example, YY isochrones adopt solar abundances from (Grevesse & Sauval 1998), while MIST isochrones employ the values from Asplund et al. (2009). Additionally, the choice of atmospheric models, such as ATLAS12, PHOENIX (BT-Settl), SYNTHE, MARCS, and others, in conjunction with the EOS, opacity values, and solar abundances, further contributes to systematic differences in the estimation of stellar ages. These differences are critical factors that must be taken into account when determining isochrone ages. They highlight the complexities and uncertainties involved in age estimation and demonstrate the need for careful consideration and

[7] https://freeeos.sourceforge.net/

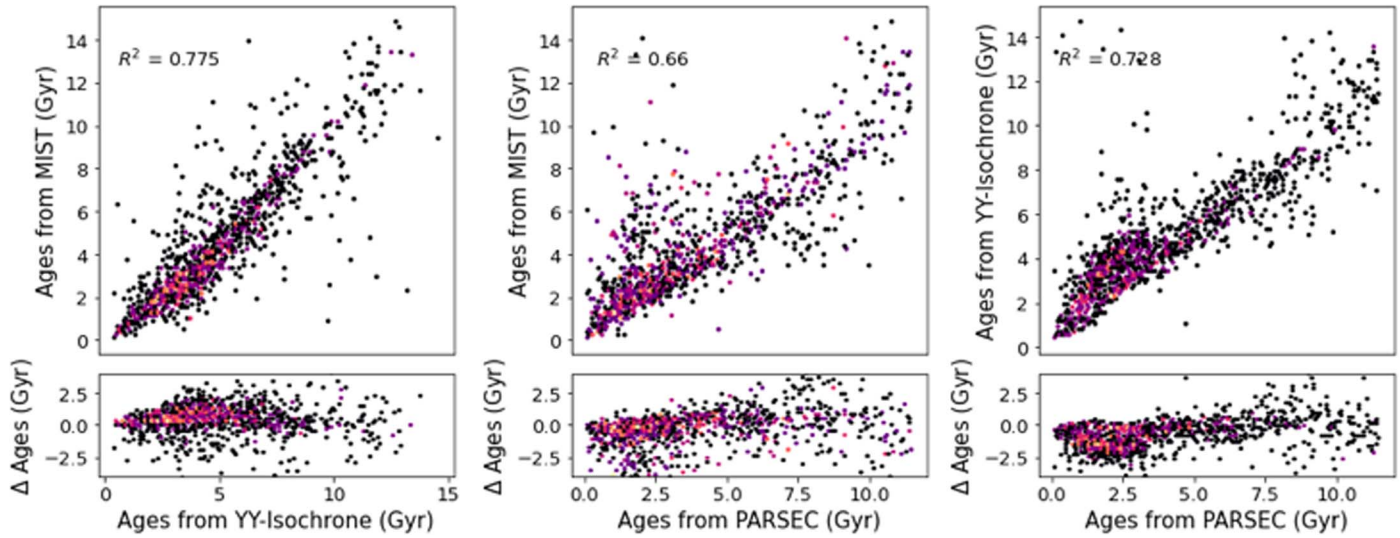

Figure 4. Comparison of stellar ages from MIST, PARSEC, and YY isochrone fitting models. The color coding represents the density of stars.

comparison of multiple isochrone models to mitigate potential biases.

We used isoclassify[8](Huber et al. 2017; Berger et al. 2020, 2023), a robust tool designed to estimate stellar ages using MIST isochrone grids. For the estimation of stellar ages using PARSEC isochrones, we used PARAM-1.5,[9] while for the YY isochrones, we used q2 tool.[10] To obtain the stellar ages, we used the observed stellar parameters such as effective temperature ($T_{\rm eff}$), luminosity (L), and metallicity ([Fe/H]) as inputs into these codes, which then matches these observations with theoretical isochrones to estimate stellar ages. To ensure the robustness of our age determinations, we conducted a comparative analysis using the age estimates derived from each of the three isochrone sets. This approach allowed us to evaluate the consistency of age estimations across different stellar models and to identify any systematic discrepancies that may arise due to the underlying assumptions of each isochrone model.

Statistical inferences drawn for a sample of stars become inherently unreliable due to the dependence of individual star age determinations on both the input parameters and the models utilized. Therefore, we estimate the ages of the stars using various models and different combinations of input parameters. Our objective is to assess whether consistent statistical conclusions could be drawn across different combinations of models and input parameters. Here, we vary certain input parameters (for instance, we use $T_{\rm eff}$ form photometry and spectroscopy) while keeping the other parameters constant (for instance using G-band magnitude and MIST isochrone models) to demonstrate how the age varies from one case to another and how the overall stellar age for the population of exoplanets varies statistically.

3.1. Choice of Stellar Temperatures

The temperature of a star is mostly obtained by spectroscopy or photometric measurements. Both of these techniques have certain assumptions while obtaining the estimate of the $T_{\rm eff}$ and this leads to a systematic difference in the estimation of ages (Wing & Yorka 1979). To verify how the input ages affect the stellar age estimates from isochrone fitting we took the $T_{\rm eff}$ from two sources: sweet-cat (Sousa et al. 2021; spectroscopic) and GAIA DR3 (Gaia Collaboration et al. 2023; photometric). Figure 2 shows the spread in age using photometric and spectroscopic temperatures using Yonsei Yale isochrone models (Han et al. 2009) and GAIA parallaxes (Lindegren et al. 2021). We find that ∼85% of the stars have an age difference <0.5 Gyr. Similarly, when employing MIST and PARSEC isochrone models, we observe that 72% and 75% of the stars, respectively show an age difference of less than 0.5 Gyr, indicating that the scatter is small with no significant systematic in the age estimates from spectroscopic and photometric temperatures.

Table 1
Sample Distribution of Stars Hosting Small and Giant Planets Used in this Paper

Count	Stellar-hosts	Planets
Total	2336	3034
Small ($M_P < 0.3M_J$)	1834	2509
Giant ($0.3M_J \leqslant M_P \leqslant 5M_J$)	502	526

Note. The above values are listed after the sample curation as described in Section 2.

3.2. Choice of Photometric-band Magnitude

The luminosity estimate in our model relies on the total flux (f), which is determined from the band magnitude provided. Given this, we explored whether the selection of photometric-band magnitudes has any noteworthy impact on the process of estimating stellar ages. We decided to use the Johnsons V-band and Gaia G-band magnitudes to estimate the ages of the exoplanet host star. Stars for which the V-band magnitude was not available, we used the relationship as described in GAIA archive[11] and used G, $G_{\rm bp}$, and $G_{\rm rp}$ magnitudes to obtain the V-band magnitude. We also tested the above relation for the stars

[8] https://github.com/danxhuber/isoclassify
[9] http://stev.oapd.inaf.it/cgi-bin/param
[10] https://github.com/astroChasqui/q2
[11] https://www.cosmos.esa.int/web/gaia-users/archive/gdr3-documentation

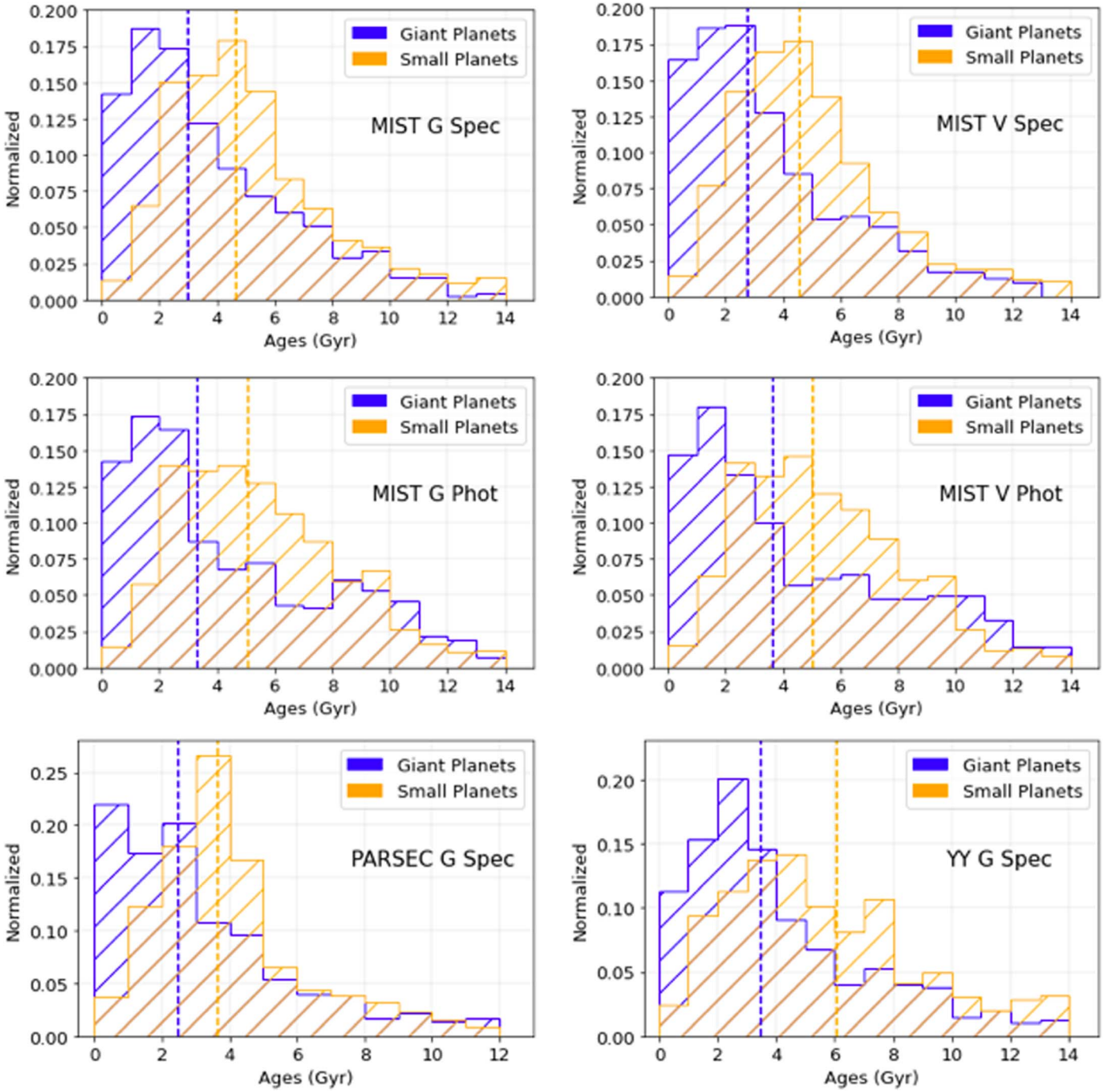

Figure 5. Histogram for ages of the planets hosting stars for small and giant planets. The label is indicated in the following format: isochrone model-photometric-band temperature from spectroscopy or photometry. The dashed lines represent the median ages corresponding to their color labels in the histograms.

whose both G band and V band were available and we found the V band obtained from the empirical relation matches with the observed ones. Figure 3 shows the correlation between the ages determined from V- and G-band magnitudes using spectroscopic temperatures and MIST. We find that the ages obtained from G band and V band are strongly correlated and do not show any significant systematic differences. We also performed this analysis with several other combinations of input parameters (for instance, using photometric and spectroscopic $T_{\rm eff}$) and did not find any considerable dispersion in any case.

3.3. Choice of Models

Most of the stellar ages obtained using isochrone use a standard stellar evolutionary isochrone fitting model to estimate the age of stars. However, the choice of the model plays an equally important role just as input parameters (Delgado Mena et al. 2019). Figure 4 shows the scatter plot in the stellar ages obtained using various isochrone fitting models using spectroscopic temperatures and G magnitude. We find that the ages estimated using MIST and YY are well in agreement, with a moderate spread but no significant systematic differences. For

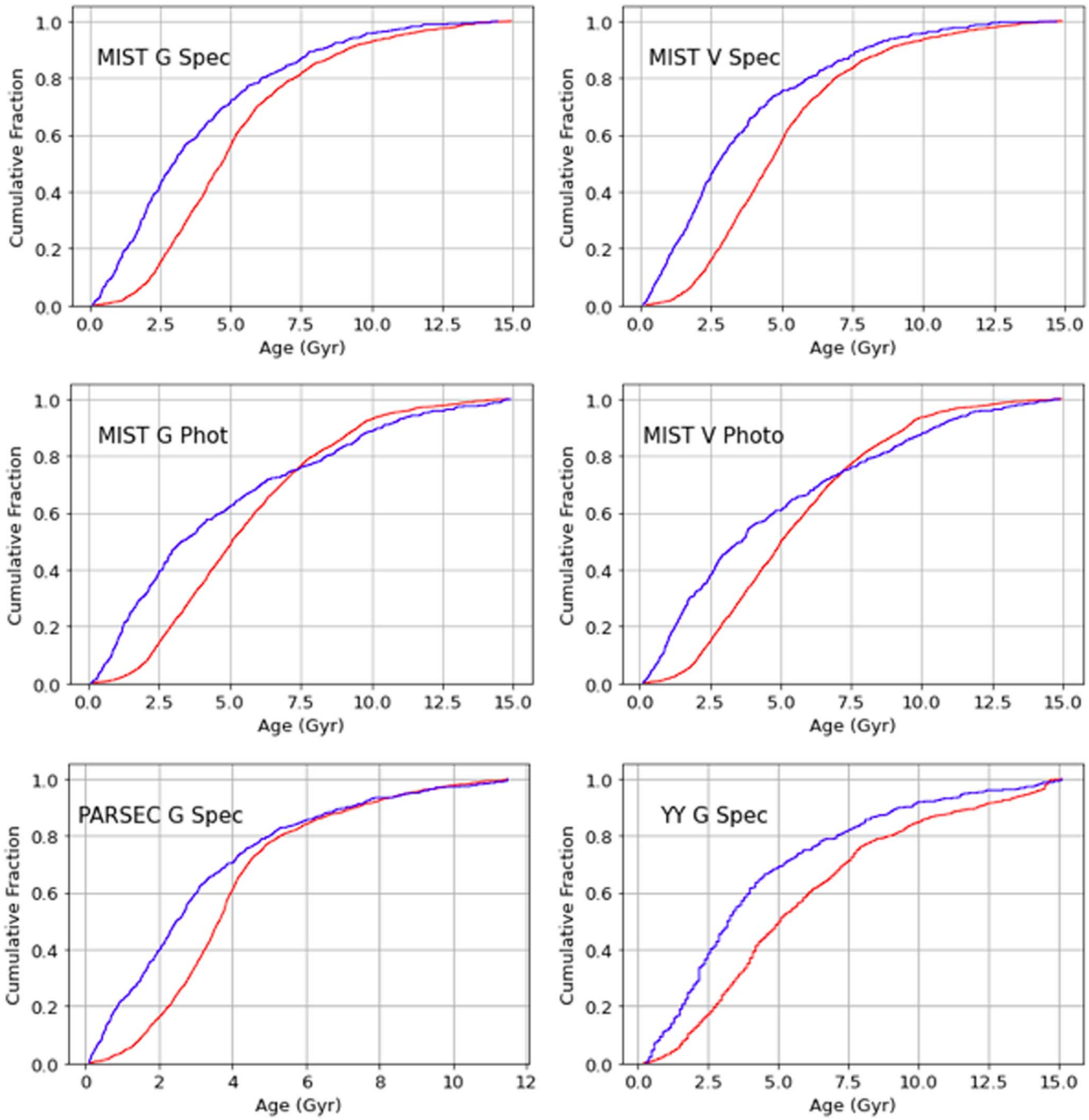

Figure 6. Cumulative distribution for the stellar ages of small (red) and giant (blue) planet-hosting stars obtained using different isochrone models and input parameters.

the stellar ages obtained using PARSEC models, we find a large scatter for stars with ages >6 Gyr, when comparing with the ages obtained using MIST and YY. We also find a notable systematic difference in the stellar ages obtained from PARSEC models when comparing the ages with MIST and YY.

4. Results

4.1. Ages of the Planet-hosting Stars

We compute the ages of the planet-hosting stars from isochrone fitting methods using different models and input parameters. Figure 5 shows the age histograms of stars hosting small planets and giant planets. Note that, even though the distribution of stellar ages computed using different models and input parameters has noticeable differences, the relative offset (median age difference) between the ages of small and giant planet-hosting stars, is always positive. In other words, the median ages of the stars hosting small planets are higher compared to stars hosting giant planets in all cases (see Table 3). We also find that the median age of stars obtained from PARSEC models is slightly lower when compared with the MIST and YY isochrone models, and this is due to the systematics of the stellar ages as obtained in Section 3.

Table 2
Comparison of Stellar Ages for the Small- and Giant-planet-hosting Stars Using Different Models and Input Parameters

	Giant Planet (Gyr)	Small Planet (Gyr)	p Value
MIST G Spec	3.00 ± 2.56	4.69 ± 2.47	10^{-26}
MIST G Phot	3.34 ± 3.12	5.08 ± 2.95	10^{-16}
MIST V Spec	2.38 ± 2.89	4.58 ± 2.37	10^{-16}
MIST V Phot	3.42 ± 3.34	5.03 ± 2.83	10^{-29}
Yonsei Y G Spec	3.45 ± 3.15	5.05 ± 2.48	10^{-36}
PARSEC G Spec	2.63 ± 2.21	3.78 ± 2.01	10^{-13}

Note. The errors quoted are the median absolute deviation in the above distributions. Here the p value obtained from the KS—test represents the probability that the two samples belong to the same distribution.

Further, the cumulative age fraction shown in Figure 6 implies that stars hosting small and giant planets belong to different populations. We also performed the Kolmogorov–Smirnov test on the sample and found that the sample of stars hosting small and giant planets fall into distinct age groups (Table 2). This result clearly suggests that small planets are common around both young and older stars, whereas giant planets are more prevalent around younger stars.

It is important to note that due to high stellar activity and radial velocity (RV) jitter,[12] the detection of small and low-mass planets around young stars is far more challenging than the detection of giant planets. Therefore, in the current exoplanet census, there is a strong possibility that some small planets might not have been detected around younger stars. However, the lack of giant planets around older stars is not likely caused by any detection or selection bias, as detecting giant planets is relatively easier than detecting small planets, regardless of the method used or the age of the star.

4.2. Planet Mass as a Function of Stellar Age

Figure 7 shows the planet-mass distribution as a function of stellar age with ∼70%–85% of stars in the sample having an age below 7 Gyr. We also note that the population of giant planets began to rise about 4–5 Gyr ago, indicating that the formation epoch of giant planets is relatively recent compared to the population of small planets, with the formation onset occurring as early as 7–8 Gyr ago. Moreover, the colorbar in Figure 7, which signifies stellar metallicity (taken from Sweet-Cat Sousa et al. 2021), reveals a metallicity gradient. This suggests that young stars that host planets are statistically richer in metals. This is also in line with the previous studies that have shown giant planet-hosting stars are metal rich (Fischer & Valenti 2005; Narang et al. 2018; Sousa et al. 2019; Swastik et al. 2022, 2023), which supports the core-accretion model for planet formation.

4.3. Planet Fraction Versus Stellar Age

In order to understand the progression of planet formation in the galaxy, we calculated the ratio of stars hosting giant planets to the stars hosting small planets as a function of the stellar age. In all cases that we analyzed in this paper, the ratio falls as a function of stellar age, as shown in Figure 8. However, It is possible that the ratio is higher for younger stars (<5 Gyr) due to selection biases and sensitivity limitations of current detection techniques. However, for stars, >5 Gyr, the finding is certainly not due to any selection or observation biases. This is because regardless of stellar type, the giant planets are easier to detect with any technique compared to the small planets. This finding possibly suggests that it is more likely that young stars have a higher ratio of giant planets to small planets when compared to older stars. A small scatter at the age bin 10–12 Gyr in Figure 8 is due to the small number of stars in that bin.

4.4. Hot Jupiters are Younger

For a subsample of the giant-planet population, we also looked at the distribution of their orbital period as a function of the ages of their parent stars obtained from different models using spectroscopic $T_{\rm eff}$ and G-band magnitude. A closer look at Figure 9 shows that the majority of these stars are young ($\leqslant$ 5 Gyr) and they are hosting hot Jupiters with orbital periods of fewer than 10 days. This is evident from the clustering of points around the lower-left sides of each plot in Figure 9. For comparison, the median age of hot Jupiters (orbital period $\leqslant$ 10 days) and warm/cool Jupiters (orbital period $>$ 10 days) is listed in Table 3. On average, the hot Jupiter hosting stars are ∼1.2 Gyr younger than the stars harboring warm/cool Jupiters.

Specifically, we note that ∼70% of giant planets have age 5 Gyr or less, indicating that overall the giant planetary systems are younger. Although the high number of young hot Jupiter (lower-left region of each plot in Figure 9) can be possibly due to detection bias as hot Jupiters are easier to detect (Kipping & Sandford 2016), we find that the number of young warm/cool Jupiters (top-left region of each plot in Figure 9) is notably higher than old hot Jupiters (bottom-right region of each plot in Figure 9), which is unlikely due to any observational bias. In fact, it again points to the scenario of the late onset of giant planet formation in the galaxy.

4.5. Isochrone versus Asteroseismology and Chemical Clock Ages

We compared the stellar ages derived from MIST isochrone models with those obtained using Asteroseismology and from α abundances (also known as chemical clocks). For Asteroseismology we used the ages from Silva Aguirre et al. (2015) and our analysis reveals that isochrone-based ages are slightly overestimated when compared to asteroseismology-derived ages as shown in Figure 10. Conversely, when comparing the ages obtained using the α abundances using the relationship in Delgado Mena et al. (2019), we find that the ages are overestimated for the younger stars ($\leqslant$4 Gyr) while they slightly underestimated for the older stars (>4 Gyr) as shown in Figure 10.

The discrepancies observed between the ages derived from MIST isochrone models, asteroseismology, and α abundances underscore the need for methodological refinement across age-determination techniques. Specifically, the tendency of asteroseismology to underestimate ages, compared to isochrone models, and the accuracy of chemical clocks for stars of different ages highlights the importance of cross validating stellar ages to identify and correct systematic biases.

[12] RV jitter is the intrinsic noise in radial velocity measurements of a star, caused by factors such as stellar activity, granulation, oscillations, and instrumental limitations. It poses challenges in detecting planets, raising the detection threshold, and introducing false positives/negatives.

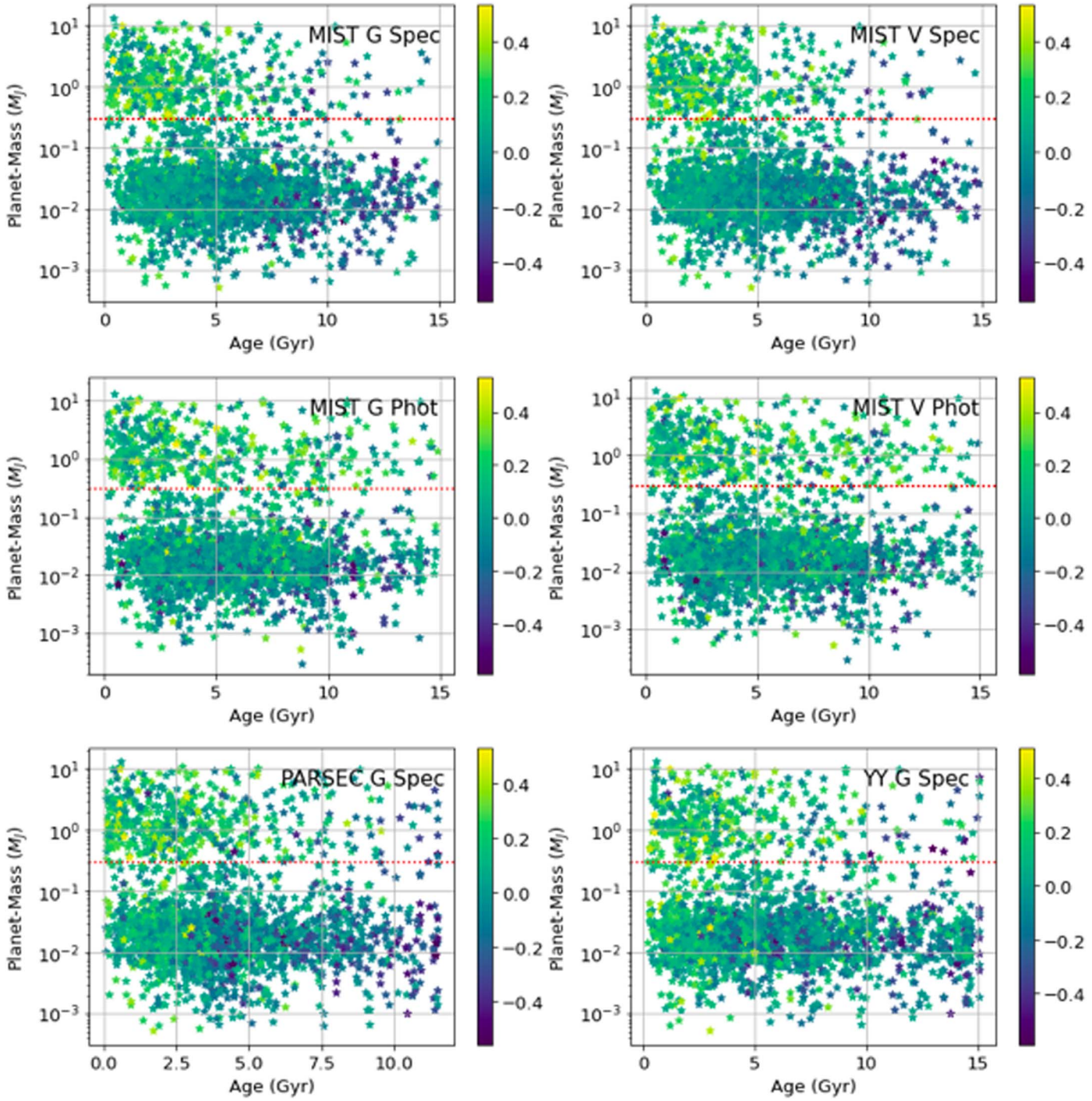

Figure 7. Planet mass as a function of stellar age. The colorbar on the right represents the stellar metallicity values obtained from the literature. The dashed red line ($M_P = 0.3M_J$) separates the small and giant planet-hosting stars.

5. Discussion

The results from Section 4 indicate that the ages for the majority of stars hosting planets are around 6–7 Gyr depending on the model. Further, within the planet's population, the giant planet-hosting stars are younger when compared to the stars hosting small planets. The reason why younger stars host more giant planets compared to older stars could be understood from the knowledge of the chemical composition and dust-to-gas ratio of their circumstellar environment. A higher dust-to-gas ratio favors the formation of giant planets (Kama et al. 2015) as: (a) The solid dust grains act as the building blocks for planetesimals and planetary cores. When the dust-to-gas ratio is higher, it means there is a larger amount of solid material available compared to the surrounding gas. This increased availability of material provides a larger reservoir for the growth and accumulation of solid cores. (b) In a higher dust-to-gas ratio environment, collisions between dust grains become more frequent. These collisions can lead to sticking and aggregation, allowing the particles to grow in size. With a greater number of collisions occurring, the growth process can proceed more rapidly, enabling the formation of larger

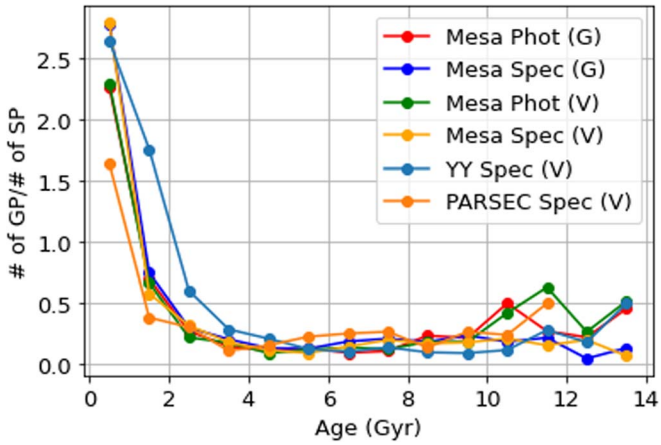

Figure 8. Fraction of stars hosting giant planets to small planets as a function of stellar age using different models and input parameters. The data is binned at an interval of 1 Gyr.

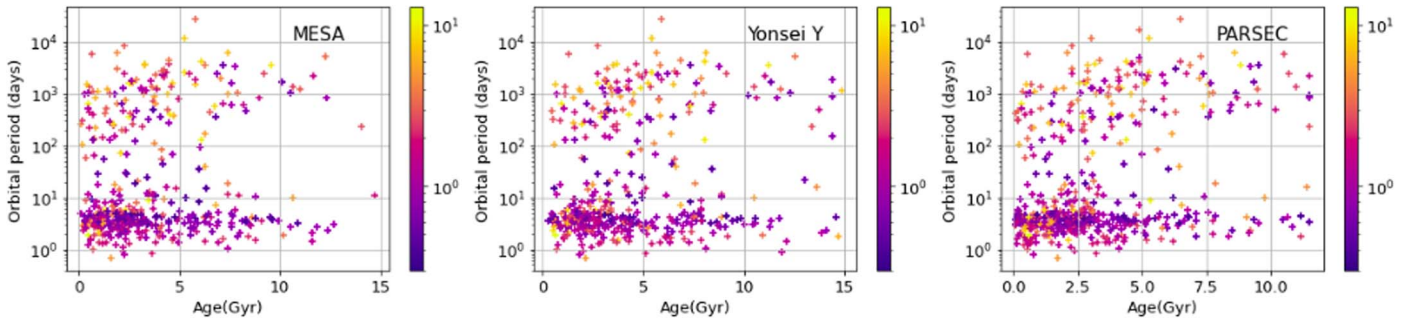

Figure 9. Distribution of giant planets as a function of stellar age. The color bars represent planet mass and labels in each plot window represent the isochrone models used. For all three cases, spectroscopic $T_{\rm eff}$ and G magnitude were used as input parameters.

Table 3
Distribution of Jupiter Hosting Stars in Terms of their Stellar Ages and Orbital Period

	Young Hot Jupiters (Count)	Old Hot Jupiters (Count)	Young Cool Jupiters (Count)	Old Cool Jupiters (Count)	Hot Jupiters (Gyr)	Cool Jupiters (Gyr)	p Value
MIST	207	60	115	46	2.43	3.50	10^{-3}
Yonsei Y	191	76	97	67	3.08	4.35	10^{-5}
PARSEC	289	48	132	56	2.15	3.38	10^{-9}

Note. The standard error of the mean is typically 0.01 Gyr for all the cases. The p-value is obtained in the same way as in Table 2.

planetesimals and planetary cores over shorter timescales (∼5–10 Myr). (c) Larger solid cores have stronger gravitational forces, enabling them to attract and capture more surrounding gas. When the dust-to-gas ratio is higher, there is a denser population of dust grains that can coalesce into larger planetesimals and cores. These more massive cores can then more effectively accrete gas from the protoplanetary disk, rapidly increasing their size and leading to the formation of gas giant planets (Emsenhuber et al. 2021; Drazkowska et al. 2023).

Together with the dust-to-gas ratio, the grain composition also plays a key role in the formation of the planetary core (Dorschner et al. 1995; Fabian et al. 2001; Draine 2003). During the early stages of galaxy evolution, the circumstellar disk is devoid of sufficient grains as the ISM is mostly enriched with Type II supernovae. The dust grains consisted of mostly silicates, magnesium, and other α but lacked iron or other heavier elements, thus resulting in a lower dust-to-gas ratio ($\ll$0.01). As the galaxy evolved, the ISM was enriched with Fe-peak elements from Type Ia supernovae, which in turn increased the dust-to-gas ratio and thus favoring the formation of both small and giant planets (Nissen 2015; Anders et al. 2018; Bedell et al. 2018; Feuillet et al. 2018; Buder et al. 2019; Delgado Mena et al. 2019). The presence of giant planets around metal-rich and young stars also correlates with higher dust-to-gas ratio (∼0.01) in young and metal-rich protoplanetary disks which makes them conducive to the formation of giant planets. This is also consistent with the core-accretion process (Pollack et al. 1996; Matsuo et al. 2007) leading to the formation of giant planet, where a solid core of ∼10–15 $M_{\oplus}$ needs to form quickly (∼10 Myr) before the gas in the disk dissipates (Haisch et al. 2001; Kraus et al. 2012), otherwise the

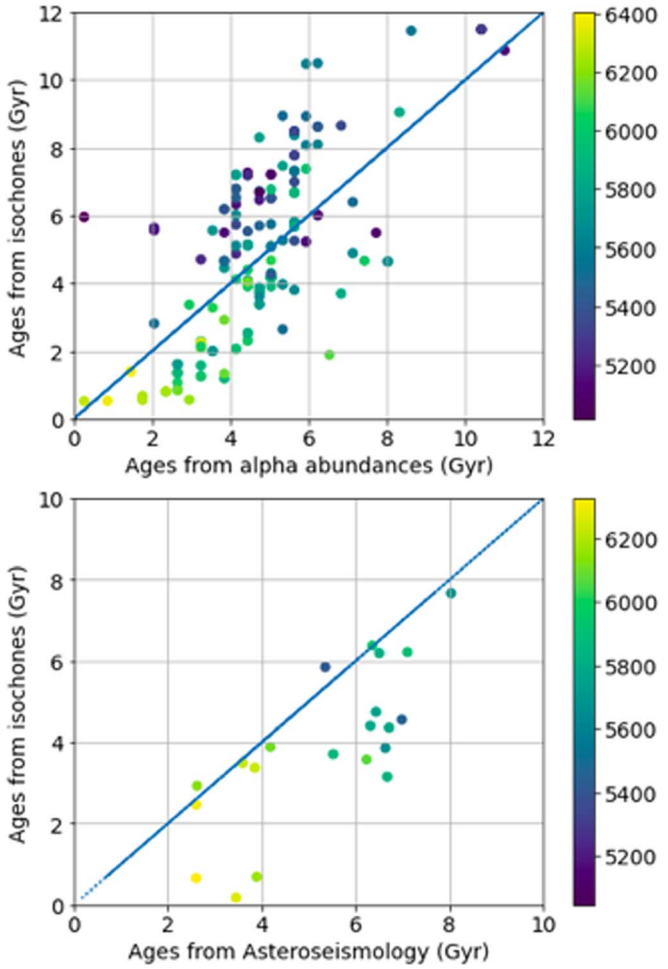

Figure 10. Top: comparison of ages obtained from stellar isochrones and from [α/Fe] abundances. Bottom: comparison of ages obtained from stellar isochrones and from Asteroseismology. The color represents the effective temperature of the star.

resulting planet would end up rocky in nature. The presence of a higher dust-to-gas ratio, thus promotes faster core formation, thereby facilitating the formation of giant planets.

6. Summary and Conclusions

The characteristics of exoplanets and their host stars exhibit a close interdependence. In the present study, we focused on estimating the stellar ages of planets orbiting main-sequence stars. To accomplish this, we used the isochrone fitting technique to estimate the stellar ages of the planet-hosting stars. Furthermore, we conducted an extensive analysis, exploring possible correlations between stellar and planetary properties to gain insights into their formation mechanisms. Our sample consisted of 2336 stars known to host planets, detected through both transit and radial velocity methods. In conclusion:

1. We computed the stellar ages for the main-sequence planets hosting stars using the isochrone fitting technique. Since isochrone ages are highly model- and input-parameter dependent, we used several models and input parameters in order to understand the systematic age differences obtained from different isochrone models.
2. We find that, even though individual age estimates and their distributions vary depending on the choice of model or input parameters, the underlying statistical trends remain unaffected.
3. Our findings suggest that 70%–85% of planets have stellar ages <7 Gyr and most of the planets started forming after the ISM was enriched sufficiently to form the cores of the planets.
4. Our analysis reveals a distinct divergence in the ages of stars hosting small planets compared to those hosting giant planets. Specifically, we observe a statistically significant age difference, with stars hosting giant planets being notably younger than those hosting small planets. This disparity suggests that the formation of Jupiter-sized planets occurred at a later stage in the galaxy's evolution, specifically when the necessary dust-to-gas ratio had reached a threshold, enabling the formation of a significant number of giant planets. These findings corroborate the core-accretion theory of planet formation.
5. Among the giant-planet population, we find that the hot Jupiters are the youngest, and they are the most recently formed systems in the context of planet formation.

In conclusion, we have analyzed the stellar ages for a large number of exoplanet-hosting stars, connecting the planet formation process to the ages of their hosts. The fact that stars hosting giant planets are younger is largely consistent with the chemical evolution of the galaxy. From the observed trends between stellar ages and planet masses, we conclude that the small planet formation started to rise after the ISM was sufficiently enriched ($\sim$6–7 Gyr), while the giant planet formation is much younger and has started to form in large numbers only in the past $\sim$4–5 Gyr.

Acknowledgments

This work has made use of (a) the NASA Exoplanet Database, which is run by the California Institute of Technology under an Exoplanet Exploration Program contract with the National Aeronautics and Space Administration and (b) the European Space Agency (ESA) space mission Gaia, the data from which were processed by the Gaia Data Processing and Analysis Consortium (DPAC) (c) the exoplanet.eu database maintained developed and maintained by the exoplanet TEAM. C Swastik would also like to thank Athul Ratnakar for the insightful discussion.

Software: Numpy (Harris et al. 2020), Topcat (Taylor 2005), Astropy (Astropy Collaboration et al. 2013), Scikit-learn (Pedregosa et al. 2011), Matplotlib (Hunter 2007), Scipy (Virtanen et al. 2020)

ORCID iDs

C. Swastik https://orcid.org/0000-0003-1371-8890
Ravinder K. Banyal https://orcid.org/0000-0003-0799-969X
Mayank Narang https://orcid.org/0000-0002-0554-1151
Athira Unni https://orcid.org/0000-0001-6093-5455
T. Sivarani https://orcid.org/0000-0003-0891-8994

References

Akeson, R. L., Chen, X., Ciardi, D., et al. 2013, PASP, 125, 989
Anders, F., Chiappini, C., Santiago, B. X., et al. 2018, A&A, 619, A125
Andreasen, D. T., Sousa, S. G., Tsantaki, M., et al. 2017, A&A, 600, A69

Asplund, M., Grevesse, N., Sauval, A. J., & Scott, P. 2009, ARA&A, 47, 481
Astropy Collaboration, Robitaille, T. P., Tollerud, E. J., et al. 2013, A&A, 558, A33
Barker, A. J., & Ogilvie, G. I. 2009, MNRAS, 395, 2268
Barragán, O., Gandolfi, D., Dai, F., et al. 2018, A&A, 612, A95
Bashi, D., Helled, R., Zucker, S., & Mordasini, C. 2017, A&A, 604, A83
Bedell, M., Bean, J. L., Meléndez, J., et al. 2018, ApJ, 865, 68
Bellinger, E. P., Hekker, S., Angelou, G. C., Stokholm, A., & Basu, S. 2019, A&A, 622, A130
Benisty, M., Bae, J., Facchini, S., et al. 2021, ApJL, 916, L2
Bergemann, M., Lind, K., Collet, R., & Asplund, M. 2011, JPhCS, 328, 012002
Berger, T. A., Huber, D., van Saders, J. L., et al. 2020, AJ, 159, 280
Berger, T. A., Schlieder, J. E., & Huber, D. 2023, arXiv:2301.11338
Binney, J., Merrifield, M., & Wegner, G. A. 2000, AmJPh, 68, 95
Bonfanti, A., Ortolani, S., & Nascimbeni, V. 2016, A&A, 585, A5
Bonfanti, A., Ortolani, S., Piotto, G., & Nascimbeni, V. 2015, A&A, 575, A18
Bressan, A., Marigo, P., Girardi, L., et al. 2012, MNRAS, 427, 127
Buder, S., Lind, K., Ness, M. K., et al. 2019, A&A, 624, A19
Carter, J. A., Agol, E., Chaplin, W. J., et al. 2012, Sci, 337, 556
Charbonneau, D., Brown, T. M., Latham, D. W., & Mayor, M. 2000, ApJL, 529, L45
Chauvin, G. 2018, arXiv:1810.02031
Choi, J., Dotter, A., Conroy, C., et al. 2016, ApJ, 823, 102
Christensen-Dalsgaard, J., & Aguirre, V. S. 2018, in Handbook of Exoplanets, ed. H. J. Deeg & J. A. Belmonte (Berlin: Springer), 184
Currie, T., Biller, B., Lagrange, A.-M., et al. 2023, in ASP Conf. Ser. 534, Protostars and Planets VII, ed. S. Inutsuka (San Francisco, CA: ASP)
Delgado Mena, E., Moya, A., Adibekyan, V., et al. 2019, A&A, 624, A78
Dorschner, J., Begemann, B., Henning, T., Jaeger, C., & Mutschke, H. 1995, A&A, 300, 503
Dotter, A. 2016, ApJS, 222, 8
Draine, B. T. 2003, ApJ, 598, 1017
Drazkowska, J., Bitsch, B., Lambrechts, M., et al. 2023, in ASP Conf. Ser. 534, Protostars and Planets VII, ed. S. Inutsuka (San Francisco, CA: ASP)
Emsenhuber, A., Mordasini, C., Burn, R., et al. 2021, A&A, 656, A70
Fabian, D., Henning, T., Jäger, C., et al. 2001, A&A, 378, 228
Feuillet, D. K., Bovy, J., Holtzman, J., et al. 2018, MNRAS, 477, 2326
Fischer, D. A., Howard, A. W., Laughlin, G. P., et al. 2014, in Protostars and Planets VI, ed. H. Beuther et al. (Tucson, AZ: Univ. Arizona Press), 715
Fischer, D. A., & Valenti, J. 2005, ApJ, 622, 1102
Gaia Collaboration, Vallenari, A., Brown, A. G. A., et al. 2023, A&A, 674, A1
Gaudi, B. S., Stassun, K. G., Collins, K. A., et al. 2017, Natur, 546, 514
Gillon, M., Triaud, A. H. M. J., Demory, B.-O., et al. 2017, Natur, 542, 456
Grevesse, N., & Sauval, A. J. 1998, SSRv, 85, 161
Haisch, K. E. J., Lada, E. A., & Lada, C. J. 2001, ApJL, 553, L153
Han, S. I., Kim, Y. C., Lee, Y. W., et al. 2009, in Globular Clusters—Guides to Galaxies, ed. T. Richtler & S. Larsen (Berlin: Springer), 33
Harris, C. R., Millman, K. J., van der Walt, S. J., et al. 2020, Natur, 585, 357
Hatzes, A. P., & Rauer, H. 2015, ApJL, 810, L25
Henry, G. W., Marcy, G. W., Butler, R. P., & Vogt, S. S. 2000, ApJL, 529, L41
Huber, D., Zinn, J., Bojsen-Hansen, M., et al. 2017, ApJ, 844, 102
Hunter, J. D. 2007, CSE, 9, 90
Iglesias, C. A., & Rogers, F. J. 1996, ApJ, 464, 943
Kama, M., Folsom, C. P., & Pinilla, P. 2015, A&A, 582, L10
Kipping, D. M., & Sandford, E. 2016, MNRAS, 463, 1323
Kraus, A. L., Ireland, M. J., Hillenbrand, L. A., & Martinache, F. 2012, ApJ, 745, 19
Lam, K. W. F., Csizmadia, S., Astudillo-Defru, N., et al. 2021, Sci, 374, 1271
Laughlin, G., & Chambers, J. E. 2002, AJ, 124, 592
Lindegren, L., Bastian, U., Biermann, M., et al. 2021, A&A, 649, A4
MacDonald, M. G., Ragozzine, D., Fabrycky, D. C., et al. 2016, AJ, 152, 105
Malavolta, L., Mayo, A. W., Louden, T., et al. 2018, AJ, 155, 107
Matsuo, T., Shibai, H., Ootsubo, T., & Tamura, M. 2007, ApJ, 662, 1282
Mayor, M., & Queloz, D. 1995, Natur, 378, 355
Mills, S. M., Fabrycky, D. C., Migaszewski, C., et al. 2016, Natur, 533, 509
Naef, D., Latham, D. W., Mayor, M., et al. 2001, A&A, 375, L27
Narang, M., Manoj, P., Furlan, E., et al. 2018, AJ, 156, 221
NASA Exoplanet Science Institute 2020, Planetary Systems Table, IPAC, doi:10.26133/NEA12
Nissen, P. E. 2015, A&A, 579, A52
Pätzold, M., Carone, L., & Rauer, H. 2004, A&A, 427, 1075
Pedregosa, F., Varoquaux, G., Gramfort, A., et al. 2011, JMLR, 12, 2825
Pollack, J. B., Hubickyj, O., Bodenheimer, P., et al. 1996, Icar, 124, 62
Pont, F., & Eyer, L. 2004, MNRAS, 351, 487
Ramírez, I., Meléndez, J., Bean, J., et al. 2014, A&A, 572, A48
Ren, B. B., Benisty, M., Ginski, C., et al. 2023, A&A, 680, A114
Rodrigo, C., Bayo, A., & Solano, E. 2017, in Highlights on Spanish Astrophysics IX, ed. S. Arribas et al. (Bilbao: Spanish Astronomical Society), 447
Saffe, C., Gómez, M., & Chavero, C. 2005, A&A, 443, 609
Santos, N. C., Israelian, G., & Mayor, M. 2004, A&A, 415, 1153
Saumon, D., Chabrier, G., & van Horn, H. M. 1995, ApJS, 99, 713
Silva Aguirre, V., Davies, G. R., Basu, S., et al. 2015, MNRAS, 452, 2127
Smith, A. M. S., Cabrera, J., Csizmadia, S., et al. 2018, MNRAS, 474, 5523
Sousa, S. G., Adibekyan, V., Delgado-Mena, E., et al. 2018, A&A, 620, A58
Sousa, S. G., Adibekyan, V., Delgado-Mena, E., et al. 2021, A&A, 656, A53
Sousa, S. G., Adibekyan, V., Santos, N. C., et al. 2019, MNRAS, 485, 3981
Swastik, C., Banyal, R. K., Narang, M., et al. 2021, AJ, 161, 114
Swastik, C., Banyal, R. K., Narang, M., et al. 2022, AJ, 164, 60
Swastik, C., Banyal, R. K., Narang, M., et al. 2023, AJ, 166, 91
Tamuz, O., Ségransan, D., Udry, S., et al. 2008, A&A, 480, L33
Taylor, M. B. 2005, in ASP Conf. Ser. 347, Astronomical Data Analysis Software and Systems XIV, ed. P. Shopbell, M. Britton, & R. Ebert (San Francisco, CA: ASP), 29
Unni, A., Narang, M., Sivarani, T., et al. 2022, AJ, 164, 181
Valls-Gabaud, D. 2014, EAS, 65, 225
Vigan, A., Fontanive, C., Meyer, M., et al. 2021, A&A, 651, A72
Virtanen, P., Gommers, R., Oliphant, T. E., et al. 2020, NatMe, 17, 261
Wahhaj, Z., Benisty, M., Ginski, C., et al. 2024, arXiv:2404.11641
Wahhaj, Z., Milli, J., Romero, C., et al. 2021, A&A, 648, A26
Wing, R. F., & Yorka, S. B. 1979, in IAU Colloq. 47: Spectral Classification of the Future, ed. M. F. McCarthy et al. (Albano Laziale: Vatican Observatory), 519
Wolszczan, A., & Frail, D. A. 1992, Natur, 355, 145
Wu, Y., Xiang, M., Chen, Y., et al. 2021, MNRAS, 501, 4917
Zhu, W., & Dong, S. 2021, ARA&A, 59, 291